Evolution of Al-Ti Oxide Inclusion during Isothermal Heating of Fe-Al-Ti Alloy at 1573 K (1300 °C)

MINGGANG LI, HIROYUKI MATSUURA, and FUMITAKA TSUKIHASHI

Evolution of Al-Ti oxide inclusion during 3 hour isothermal heating of Fe-Al-Ti alloy at 1573 K (1300 °C) was studied. Homogeneous spherical Al-Ti oxide inclusion with nonstoichiometric composition was observed in two as-cast alloys. After heating, most of the homogeneous Al-Ti oxide inclusions changed to heterogeneous ones with Al-rich and Ti-rich parts, while the remaining homogeneous oxides were rare in both alloys. The concentration gradient of Al and O was observed inside the heterogeneous inclusion. The size distribution extended more broadly, and the shape changed from spherical to irregular. The mechanism of the variation was proposed as the diffusion of Al and O in the homogeneous inclusion from the inside to the surface of inclusion to precipitate alumina during heating.

DOI: 10.1007/s11663-017-0968-y

I. INTRODUCTION

PRECISE process control from raw material to final product is required for the production of high-grade steel. Plenty of research has been conducted on the behavior of nonmetallic inclusions in molten steel and during solidification. However, the number density, composition, or morphology of inclusions may vary during the following reheating and rolling process. Knowledge of the evolution of inclusions during heating in solid steel is still insufficient.

Al-Ti oxide inclusion has gained great attention by researchers, as it is frequently generated from the Al and Ti deoxidation process adopted in the production of automobile sheets, heavy plates, and pipeline steels. Al-Ti oxide inclusion has been studied well at the molten steel temperature. Nevertheless, the discrepancies of the thermodynamic description of the Al-Ti-O system in molten iron still remain due for the following reasons: (1) Ti forms many types of oxide, as it has more than one stable valence state; (2) the reciprocal solubility between Al_2O_3 and TiO_x results in the complexity of stable phase, and available literature studies are not in agreement with each other; and (3) thermodynamic modeling is performed on the limited experimental data. Moreover, the existence of a liquid oxide phase in the Fe-Al-Ti-O system has remained an open question due to the lack of phase equilibrium data for the Al-Ti-O ternary system, especially at low oxygen partial pressures. Ruby-Meyer *et al.*[1] employed the multiphase equilibrium code CEQCSI based on the IRSID slag model to calculate the Fe-Ti-Al-O equilibrium phase diagram at 1793 K (1520 °C), assuming Ti_2O_3 as the stable oxide. The calculated diagram indicates the formation of Al_2O_3, Ti_2O_3, and Al_2TiO_5 as well as Al_2O_3-TiO_x liquid oxide. On the other hand, Jung *et al.*[2] used the FactSage database to calculate the same equilibrium phase diagram at 1873 K (1600 °C), considering the existence of Ti_3O_5 solid phase as well as Ti_2O_3. Later, they revised the previous phase diagram in which Al_2O_3, Ti_2O_3, Ti_3O_5, and a liquid oxide equilibrate with metal. They also pointed out the existence of a liquid Al-Ti-O phase with unfixed Al/Ti molar ratio at 1873 K (1600 °C).[3] The transient behavior of Al-Ti oxide in liquid iron has also been investigated by many researchers.[4–8] The final inclusions were found to be greatly affected by Ti sources, the order of Al and Ti addition, and the ratio of Al to Ti. Wang *et al.*[8] suggested that the formation of liquid Al-Ti oxide phase with nonstoichiometry should be considered, as well as the need for experimental data to prove its existence in the research for the reoxidation effect on transient oxide evolution. However, this question is still unaddressed by any experimental study up to now.

Choi *et al.*[9,10] studied the effect of nitrogen on the behavior of inclusions in Fe-Al-Ti-O-N-S alloy during heating at 1473 K (1200 °C), and the TiN-based inclusions were found to retard grain growth more effectively than TiS-based inclusions. However, neither the equilibrium data or the evolution behavior of Al-Ti oxide inclusion in solid steel temperature has been clarified yet.

The present study aims to clarify the evolution of Al-Ti oxide inclusion during isothermal heating of Fe-Al-Ti alloy at 1573 K (1300 °C). The composition and morphology variation of inclusions during heating was characterized using scanning electron microscopy/energy-dispersive spectroscopy.

II. EXPERIMENTAL

A. *As-Cast Alloy Preparation*

Alloys 1 and 2 with the different ratios of Al to Ti content shown in Table I were made by the following

MINGGANG LI, HIROYUKI MATSUURA, and FUMITAKA TSUKIHASHI are with the Graduate School of Frontier Sciences, The University of Tokyo, 5-1-5 Kashiwanoha, Kashiwa, Chiba, 277-8561, Japan. Contact e-mail: matsuura@material.t.u-tokyo.ac.jp
Manuscript submitted November 9, 2016.
Article published online March 30, 2017.

procedure: 120 g of electrolytic iron were melted in an MgO crucible (OD: 40 mm, ID: 28 mm, and H: 100 mm) under Ar-3 pct H_2-N_2 gas atmosphere by an induction furnace (200 kHz, approximately 3 kW) at 1873 K (1600 °C). Then, about 0.1 g of aluminum (purity 99.9 mass pct) and 0.06 g of titanium (purity 99.9 mass pct) were added into the melt with an interval of 2 minutes, and the melt was further maintained for 3 minutes before quenching into water. Chemical compositions were analyzed by inert gas fusion impulse infrared absorption spectroscopy for total oxygen content, the inert gas fusion thermal conductivity method for total nitrogen, and Inductively coupled plasma optical emission spectrometry (ICP-OES, SPS7800, Seiko Instruments Inc., Japan) for soluble Al and Ti. It is noted that the chemical homogeneity of as-cast alloys was carefully checked by analyzing samples cut from three different positions from top to bottom.

The compositions of two alloys are plotted on the phase stability diagram of oxide phases equilibrated with Fe-Al-Ti-O melt at 1873 K (1600 °C), as shown in Figure 1.[11] It is noted that the calculation of this phase diagram is based on the consideration of Ti_2O_3, Ti_3O_5, and Al_2TiO_5 as the existing phases. Al_2O_3 is found to be the stable phase for these two alloys. It is worthwhile noting that the compositions of alloys are close to the Al_2TiO_5 stable area in which arguments of the existence of a liquid phase remain.[1,3,5–8]

B. *Heating Experiment*

A piece of alloy sample was cut from the cylindrical as-cast alloy including the whole part from the edge near the crucible to the center and sealed in a quartz tube (ID: 8 mm, OD: 9 mm, and L: 30 to 40 mm) with evacuated atmosphere to prevent oxidation during heating. The samples were heated in the electric resistance furnace shown in Figure 2 for 3 hours at 1573 K (1300 °C). A working thermocouple was placed adjacent to the sample to measure the actual temperature of the sample. The temperature deviation was ±3 K (±3 °C) during heating. The Ar stream with 1 L/min was introduced from the bottom. After a prescribed time, the quartz tube was taken out quickly and broken up to quench the alloy piece into water within 10 seconds.

C. *Inclusion Characterization Method*

As-cast and heated samples were embedded in resin, and then they were polished by SiC papers and diamond suspensions up to 0.25 μm to characterize the inclusions by a field scanning electron microscope (S4200, HITACHI, Japan) equipped with a silicon drift X-ray detector (energy-dispersive spectrometer, HORIBA EMAX, Japan). The analysis was conducted with an accelerating voltage of 10 kV, working distance of 15 mm, and emission current of 10 μA. The concentrations of inclusions were determined by point analysis according to the extended Pouchou and Pichoir algorithm, and element distribution was examined by mapping analysis. The Fe signal from the matrix was collected by a detector to deliver the original composition of inclusions. The description of inclusions as "$X + Y$" means there are two different X and Y phases in one particle, whereas "$X-Y$" denotes a single phase composed of two components in both as-cast alloys. The description of $X-Y$ is maintained as Al-Ti oxide before

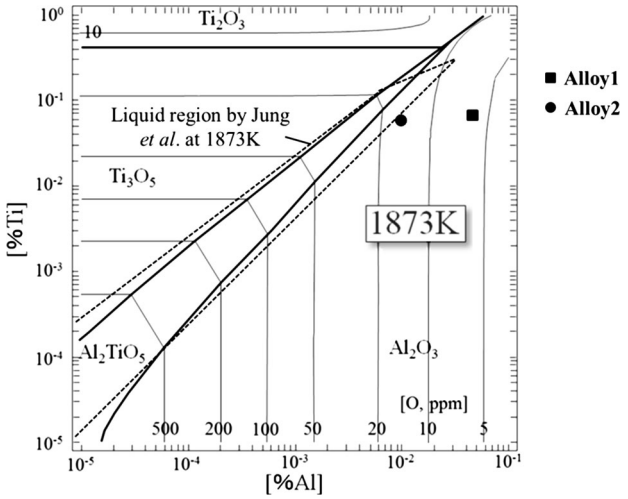

Fig. 1—Compositions of alloys on the calculated phase stability diagram for oxides in equilibrium with Fe-Al-Ti-O melt at 1873 K (1600 °C).

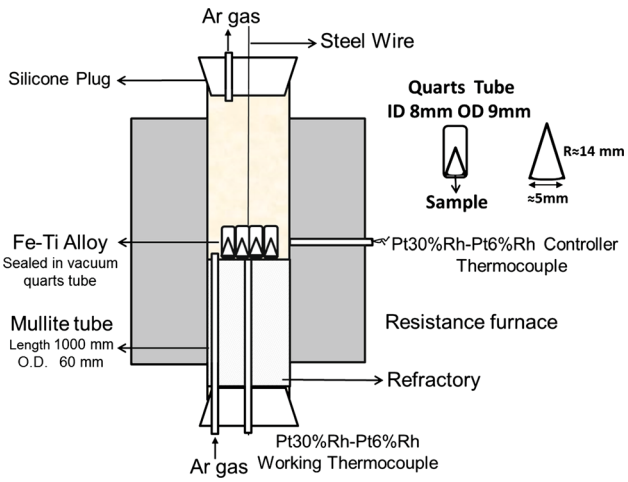

Fig. 2—Schematic of apparatus setup for heating experiment.

Table I. Composition of Alloys

Alloy	Soluble Al (Mass Pct)	Soluble Ti (Mass Pct)	Total O (Mass Pct)	Total N (Mass Pct)	Al/Ti (Molar Ratio)
1	0.0497	0.0636	0.0020	0.0032	1.4
2	0.0123	0.0586	0.0069	0.0110	0.4

heating, even it is heterogeneous phase in two heated alloys, to distinguish it from Al + Ti oxide.

The morphology of inclusion was determined by secondary electron images (SEIs) with magnification ranging from 5000 to 80,000 times. The size of inclusion was denoted by the maximum length of one particle.

III. RESULTS AND DISCUSSION

The inclusion observation area was divided into two layers, the same as in the previous research conducted by Choi *et al.*[9] In the outer layer near the crucible wall, oxides were mainly found, while in the inner layer, titanium nitrides were predominantly discovered in both as-cast and heated alloys. The difference was attributed to the inductive force during the preparation of as-cast alloys. Three types of oxide inclusions were found in the outer layer in both as-cast and heated alloys: Al_2O_3, Al + Ti oxide, and Al-Ti oxide.

A. *Characterization of Inclusions in the As-Cast Alloys*

The distribution characteristics of these three oxides differed, as shown in Figure 3. A similar distribution was observed in both as-cast and heated alloys. The magnified figures of each oxide are presented in Figures 4(a) through (c), and the mapping analysis result of the Al-Ti oxide inclusion is demonstrated in Figure 4(c). The general findings are summarized as follows.

(a) Al_2O_3 inclusion was the oxide inclusion mostly found near the crucible wall. It was formed as a deoxidation product after Al addition, and the morphology was irregular.
(b) Al + Ti oxide was distributed in the area close to Al_2O_3 inclusion. The mapping results showed a dual phase of alumina core with Ti-rich layer. These findings agreed with the results of transient inclusion evolution in Fe-Al-Ti-O melts,[4–8] in which the same type of inclusions were formed after Ti addition in an Al-deoxidized melt. The morphology of Ti-rich layer is spherical than irregular, indicating the formation of liquid phase.
(c) Al-Ti oxide was found to be dispersed on the area apart from Al_2O_3 inclusion (Figure 4(a)) and Al + Ti oxide (Figure 4(b)), inferring the different formation mechanism. Each particle has spherical morphology, as shown in Figure 4(c). Besides the dispersed ones, alignment of spherical oxides presenting the gradual change from relatively larger to smaller oxides was also observed, as shown in Figure 5. The direction of aligned oxides was random. The size of most Al-Ti oxides ranged from 0.5 to 1.5 μm. The size distribution of these oxides is explained in later discussion.

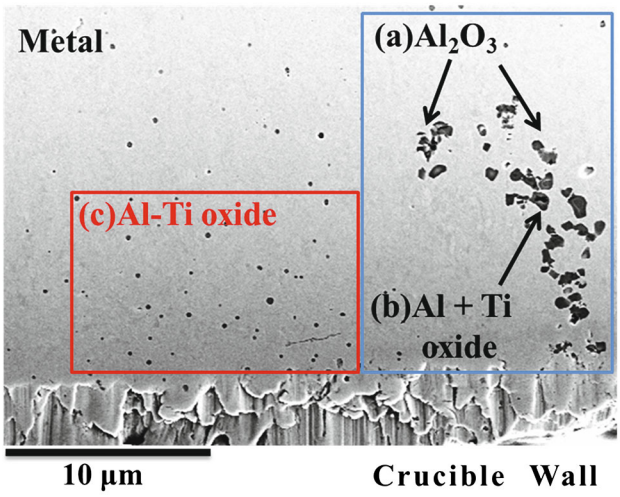

Fig. 3—Overall distribution of three types of oxide inclusions: (*a*) Al_2O_3, (*b*) Al + Ti oxide, and (*c*) Al-Ti oxide.

Spherical inclusions were normally considered as liquid phase; nevertheless, this is not a verdict. Steinmetz *et al.*[12] proposed that solid alumina inclusion with spherical shape was favored to form under a high ratio of oxygen to aluminum content in a static melt condition. The as-cast alloys were prepared in a dynamic melt affected by inductive force in the present experiment. However, directional alignment of inclusions cannot be formed given the solid phase in melt. Therefore, the spherical Al-Ti oxide was considered as liquid phase in the melt at 1873 K (1600 °C). The unidirectionally aligned oxides are formed because original big oxide inclusions can be easily smashed into smaller ones by strong turbulence. Moreover, chemical homogeneity was observed inside these oxide inclusions from the mapping analysis results shown in Figure 4(c).

The composition of Al-Ti oxides in both alloys is plotted onto the Al-Ti-O diagram after normalization, as shown in Figure 6. At least 30 oxide inclusions were analyzed in each as-cast alloy. The Al/Ti molar ratio of inclusions was 1.4 in alloy 1 and 0.3 in alloy 2, whereas the oxygen concentration fluctuated due to inaccurate quantitative analysis to light elements by EDS. The Al/Ti molar ratio of Al-Ti-O inclusions was consistent with that of alloy in both cases, suggesting the fast mass transfer between liquid inclusion with melt at 1873 K (1600 °C).

In the research regarding the effect of Ti/Al ratio on transient inclusions in Fe-Al-Ti-O melts conducted by Wang *et al.*,[6] the homogeneous spherical Al-Ti oxides were also found in the melt whose composition is adjacent to the Al_2TiO_5 steady area on the oxide phase diagram, and their existence was confirmed after sufficient holding time. The final composition of these oxides showed a discrepancy from the expected Al_2TiO_5 phase, demonstrating the limitation of the assumption that Al_2TiO_5 was solely stable phase. Upon further investigation of the effect of reoxidation on transient inclusions, these homogeneous spherical Al-Ti oxides were found to be dominant until the experimental end stages.[8] In Wang *et al.*'s research, the morphology of Al-Ti oxides was not studied in detail, and the composition was determined based on the X-ray signal of Al, Ti, and O without considering Fe by measurement of the detector, which may lose the original composition of

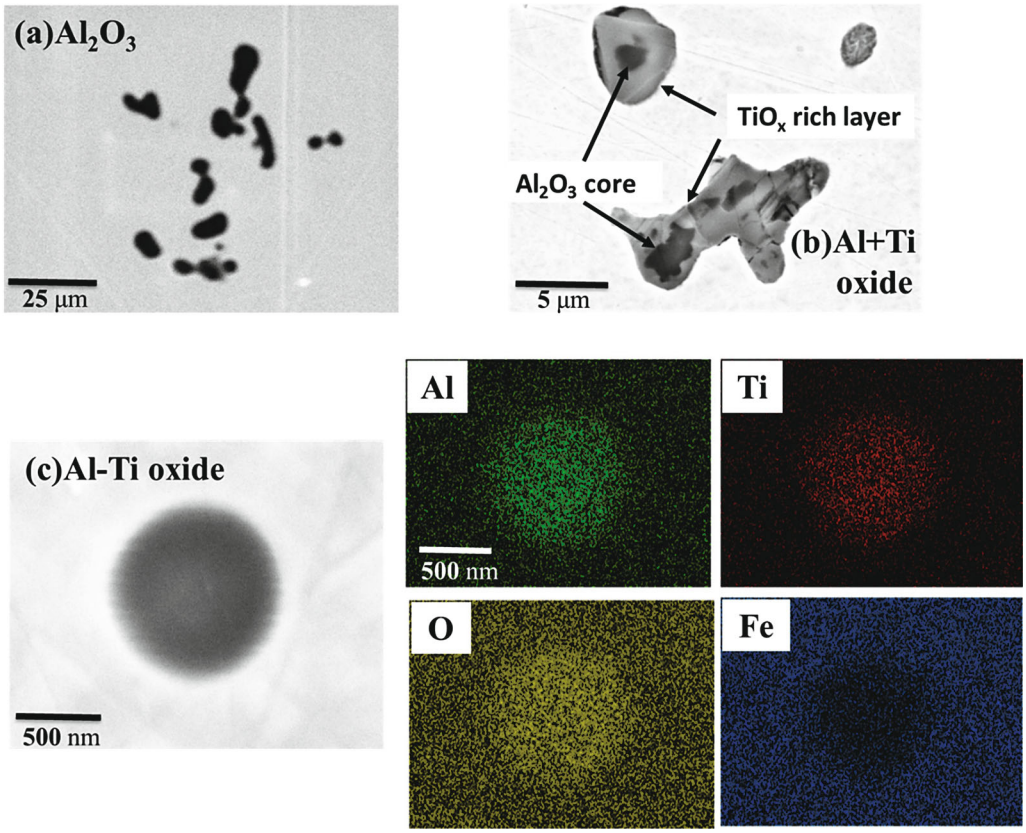

Fig. 4—Magnified images of each oxide from (*a*) to (*c*) and mapping analysis result of Al-Ti oxide.

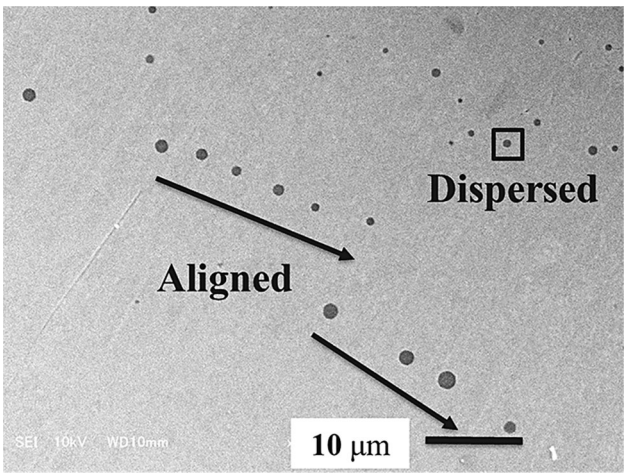

Fig. 5—Dispersed and unidirectionally aligned Al-Ti oxides.

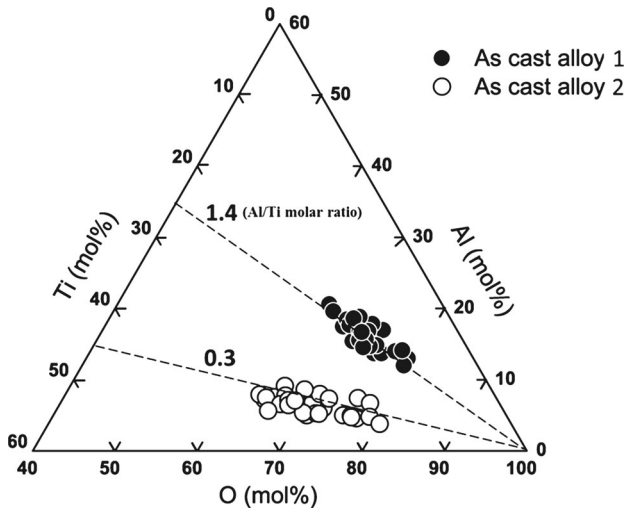

Fig. 6—Composition of Al-Ti oxide inclusions plotted on the Al-Ti-O diagram.

these oxides; thus, the corresponding composition relation between oxides and metal was neglected. Therefore, the identification of these oxides was still uncertain, although they have been observed in previous studies. However, Wang *et al*. proposed that a liquid oxide phase with unfixed stoichiometry between Al_2O_3 and TiO_x should be considered, besides Al_2TiO_5.[8] Moreover, Jung *et al*.[3] presented the area of this liquid phase in the Fe-Ti-Al-O equilibrium phase diagram at 1873 K (1600 °C) by the optimization of thermodynamic data.

Based on the morphology investigation and corresponding composition relationship between Al-Ti oxides and alloy in the current research, the spherical Al-Ti oxides were considered as a stable phase attaining local equilibrium with melt at 1873 K (1600 °C). This result agrees with the argument of the existence of a liquid phase in the Fe-Al-Ti-O phase diagram at 1873 K

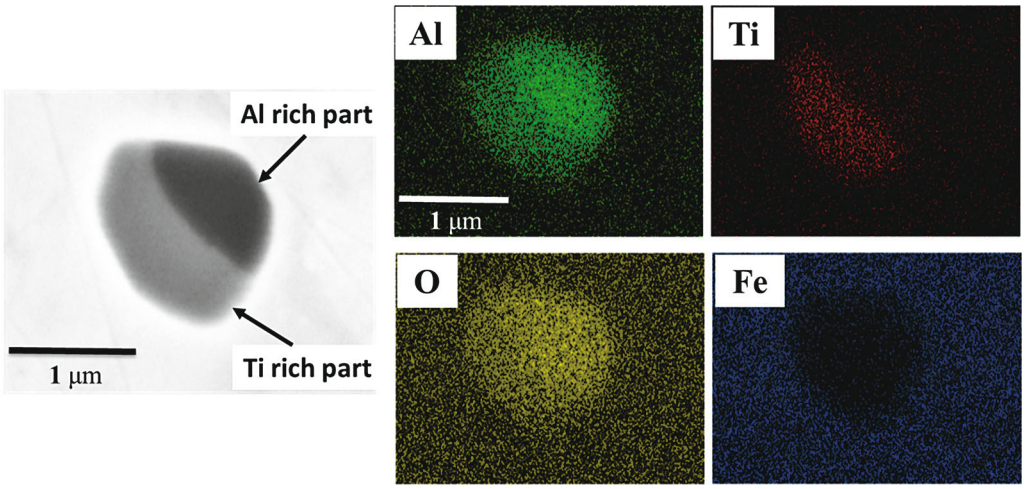

Fig. 7—Mapping analysis results of Al-Ti oxide inclusion after heating.

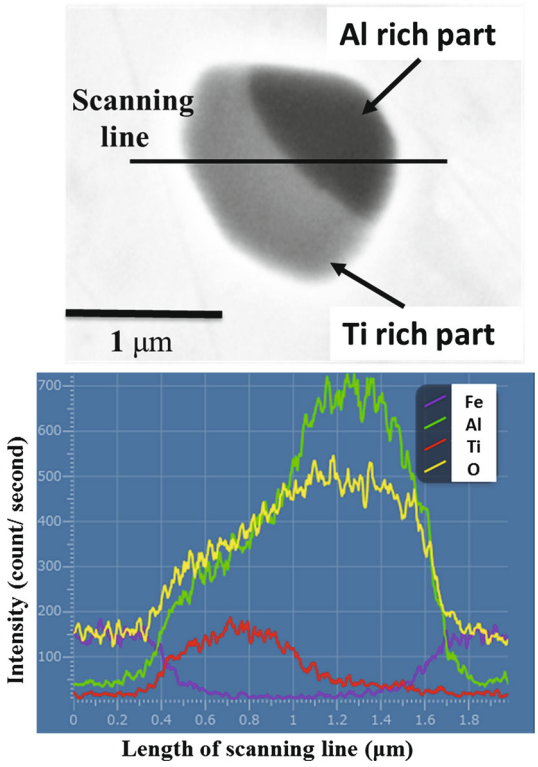

Fig. 8—Scanning line analysis result of heterogeneous oxide.

(1600 °C). However, it is hard to experimentally prove the existence of these Al-Ti oxides as equilibrium phase.

B. *Evolution of Al-Ti-O Oxide Inclusion during Isothermal Heating*

The different distribution characteristics between Al-Ti oxides and Al + Ti oxides in both as-cast and heating samples enable analysis of the same type of oxides after heating. The homogeneous Al-Ti oxides in cast alloys were found to change to heterogeneous ones during heating, and this behavior was characterized by

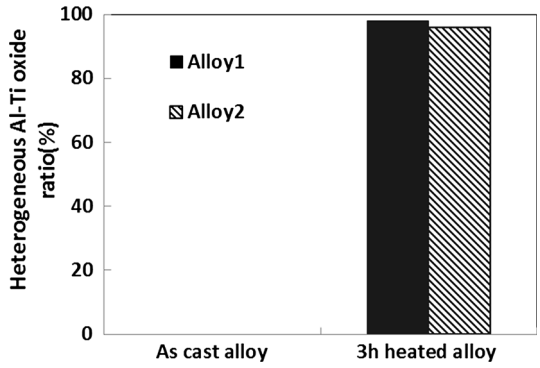

Fig. 9—Ratio of heterogeneous oxide before and after heating 3 h at 1573 K (1300 °C).

the composition and morphology of inclusions. The Al + Ti oxides may also follow the same changing discipline during heating; however, they were not characterized in this research, as they maintained dual phase after heating.

1. *Composition change*

The most homogeneous Al-Ti oxides changed to heterogeneous ones after heating in both alloys, and the mapping analysis results are shown in Figure 7. The particle could be divided into two parts: the Al-rich part, in which Al was only observed, and the Ti-rich part, in which Ti coexisted as the main element with Al. In the SEI image, the Al-rich part was black while the Ti-rich part was gray.

The heterogeneous oxide after heating was analyzed by a scanning line, as shown in Figure 8. It is of interest to determine if Al and O concentration gradients exist within the Ti-rich part of the particle with width around 1 μm. The Ti concentration gradient width in the Al-rich part exists around 0.4 μm. The quantitative spatial analysis depth of EDS under the present experimental condition is calculated to be 0.4 μm employing the Castaing equation, and 3.702 is adopted as the density of the Ti-rich part for calculation by assuming its phase

Table II. Number of Homogeneous and Heterogeneous Al-Ti Oxide Observed in Two As-Cast and Heated Alloys

Alloy	Condition	Homogeneous Oxide	Heterogeneous Oxide
1	as cast	101	0
	heated	2	78
2	as cast	100	0
	heated	3	73

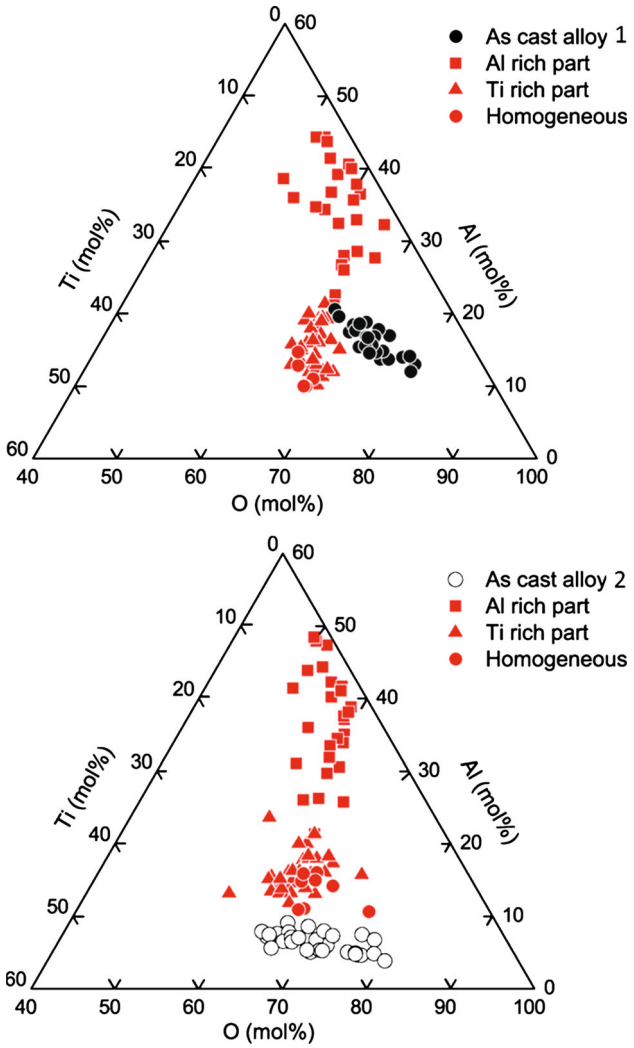

Fig. 10—Composition of Al-rich and Ti-rich parts and homogeneous oxides.

is Al_2TiO_5.[13] Therefore, the Ti concentration gradient in the Al-rich part results from the EDS analysis limitation rather than the nature of oxide. The same behavior was observed in both alloys.

It is worth noting that there were still oxides in which Al and Ti distributed almost homogeneously, such as the ones in the as-cast alloys shown in Figure 4(c), while the shape differed slightly from spherical. For two heated alloys, the ratio of heterogeneous oxide to homogeneous oxide before and after heating 3 hours at 1573 K (1300 °C) is shown in Figure 9. The number of homogeneous and heterogeneous Al-Ti oxides observed in two as-cast and heated alloys is shown in Table II. As the overall changing trend is the same, from 30 to 40 Al-Ti oxides were analyzed by EDS randomly in each heated alloy, and the compositions of the Al-rich part, Ti-rich part, and homogeneous oxides are shown in Figure 10. The Al/Ti molar ratio of the Al-rich part and Ti-rich part presented deviation from that of homogeneous oxides in cast alloy 1. The Al/Ti molar ratio of the Ti-rich part was slightly larger while that of the Al-rich part was much larger than that of homogeneous oxides in cast alloy 2. The concentration of Al in the Ti-rich part of the heterogeneous oxides in alloy 2 after heating was relatively low and the oxide size was around 1 μm; therefore, the Al X-ray signal originating from Al would be easily affected by the Al gradient toward the Al-rich part. The composition of the Al-rich part in two heated alloys was close to alumina, and the Ti detected in the Al-rich part was considered to be generated from the Ti-rich part. The composition of homogeneous oxide overlapped with that of the Ti-rich parts.

2. *Morphology change*

In addition to the spherical-like shape, the irregular shape and bar shape oxides were also observed in both heated alloys, as shown in Figures 11(a) and (b). Moreover, the Al-rich part between two Ti-rich parts inside one particle, as illustrated in Figure 11(c), and the occurrence of the Al-rich part in both the surface and inner parts of one oxide, shown in Figure 11(d), were found, indicating the formation of the Al-rich part from the oxide inclusion itself.

Figure 12 presents the distribution of the size of Al-Ti oxides in as-cast alloys and heated alloys. Eighty to one hundred oxides were observed for both as-cast and heated alloys, including homogeneous ones in each alloy. The size of Al-Ti oxides is around 1 μm. The converging distribution characteristics of size were found to maintain after heating. However, the size distribution extended more broadly after heating in both alloys as the result of morphology variation from spherical to irregular.

C. *Mechanism of Variation of Al-Ti Oxide Inclusion During Heating*

Suppose the change is caused by reaction between the oxide inclusion and alloy matrix during heating, a reaction layer with ring shape would be favorably formed, which contradicts the morphology of heterogeneous oxide inclusion after heating.

Based upon the experimental results presented previously, the mechanism of variation of Al-Ti oxide inclusion is proposed, as illustrated in Figure 13. During heating, the Al and O in the homogeneous oxide inclusion diffuse from the inside to the surface of inclusion to precipitate alumina through heterogeneous nucleation. Therefore, Al and O concentration gradients were observed, as shown in Figure 8. The simultaneous observation of heterogeneous and homogeneous oxides

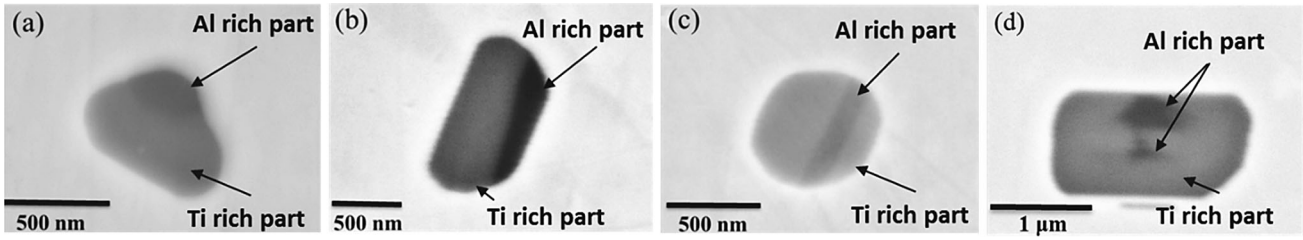

Fig. 11—(*a*) Irregular and (*b*) bar shape of the oxides after heating and (*c*) and (*d*) Al-rich part (black color) generated between two Ti-rich parts inside one particle.

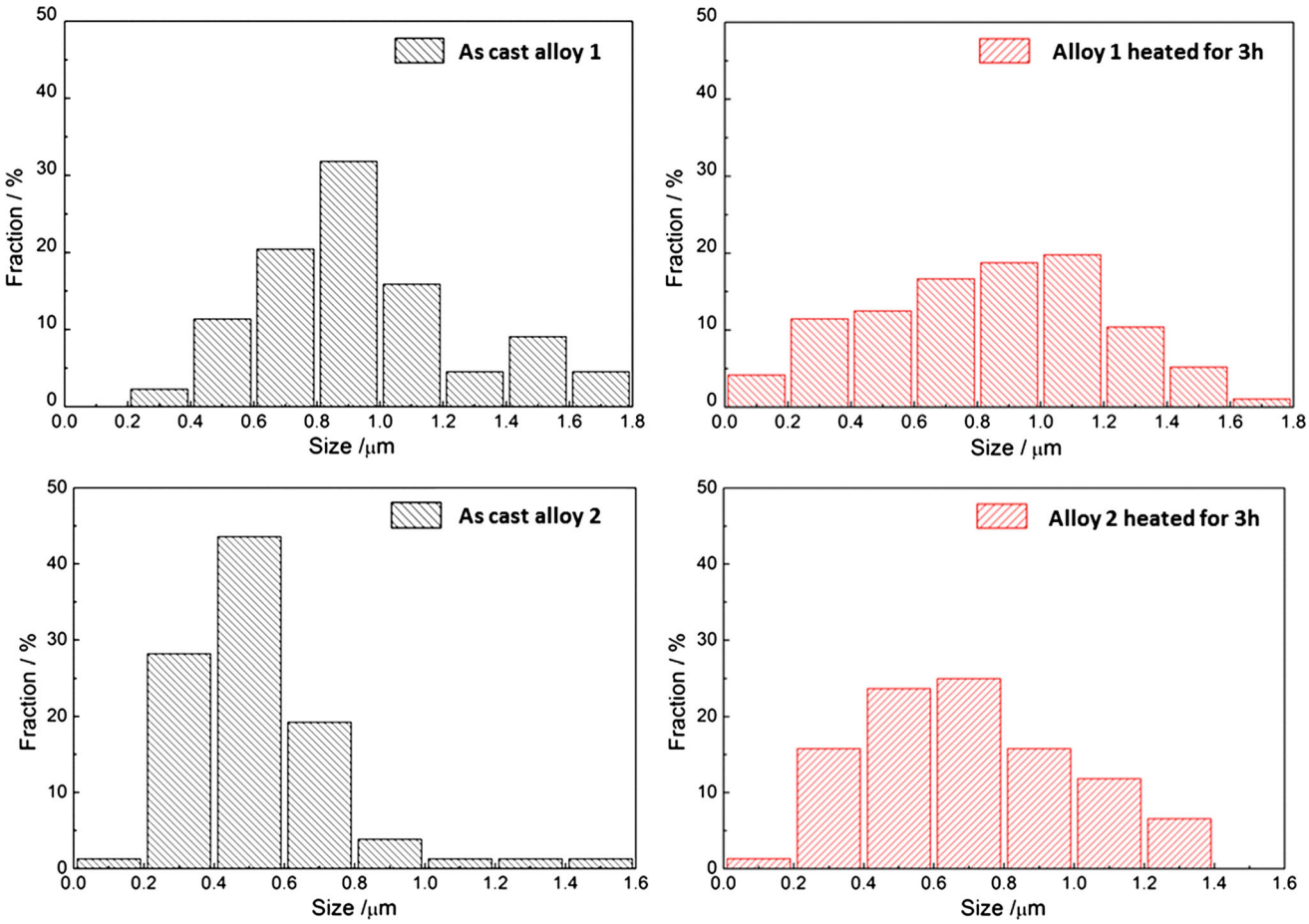

Fig. 12—Size distribution of Al-Ti oxides in as-cast and heated alloys.

in heated alloys results from the two-dimensional inclusion characterization method in the current research. The heterogeneous ones were observed by the exposed section crossing both the Al-rich and Ti-rich parts, while the homogeneous ones were analyzed through the exposed section of the Ti-rich part.

Due to the lack of thermodynamic data of the Al-Ti-O-Fe system at 1573 K (1300 °C), the result was compared with the reported calculating diagram[3] through the FactSage thermodynamic modeling technique. Several assumptions are made as follows: (1) Al and Ti in oxide inclusion exist as Al_2O_3 and Ti_2O_3 phase, respectively; (2) oxygen in liquid alloy is equilibrated with both Al-Ti oxide inclusion and atmosphere at 1873 K (1600 °C); and (3) the oxygen partial pressure equilibrated with oxide inclusion at 1573 K (1300 °C) is the same as that at 1873 K (1600 °C).

The equilibrium between oxygen gas and dissolved oxygen in the liquid alloy is shown in Eq. [1].[13]

$$\frac{1}{2}O_2(g) = \underline{O}\ (\text{mass pct})$$

$$\Delta G^\circ = -117110 - 3.39T\ \text{J/mol} \qquad [1]$$

The oxygen partial pressures equilibrated with liquid alloy were calculated from the analyzed total oxygen contents employing interaction coefficients $e_O^{Al}(-1.17)$, $e_O^{Ti}(-1.12)$, $e_O^{O}(-0.17)$, and $e_O^{N}(-0.14)$ in liquid iron at

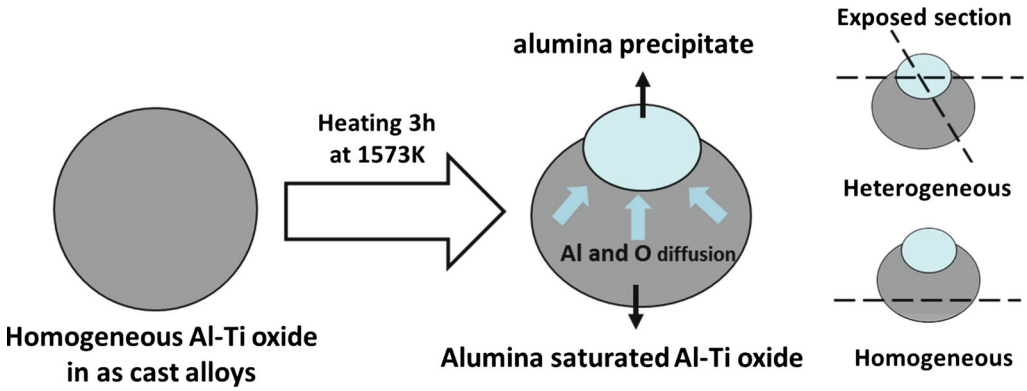

Fig. 13—Mechanism of variation of Al-Ti oxide inclusion during heating.

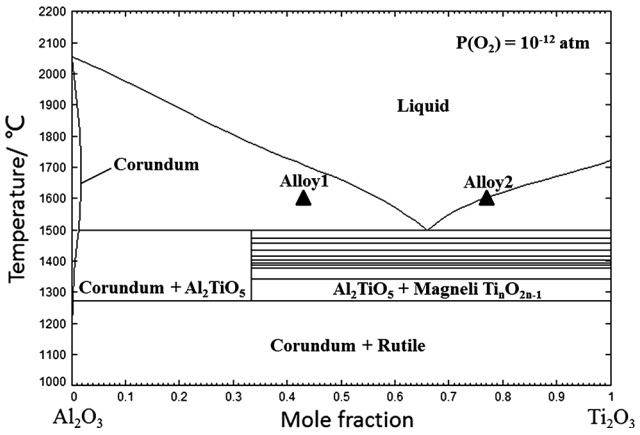

Fig. 14—Calculated phase diagram of Al_2O_3-Ti_2O_3 system at $P_{O2} = 10^{-12}$ atm.

1873 K (1600 °C).[14] The obtained values were 3×10^{-13} and 4.2×10^{-12} atm for alloys 1 and 2, respectively. Figure 14 shows the calculated phase diagram of the Al_2O_3-Ti_2O_3 system at $P_{O2} = 10^{-12}$ atm, and compositions of Al-Ti oxide inclusion in two alloys are plotted on it. According to the phase diagram, the Al-Ti oxide inclusion exists as liquid phase in both alloys at 1873 K (1600 °C). However, Al_2TiO_5 + Magneli Ti_nO_{2n-1} are found to be stable phase at 1573 K (1300 °C). Notably, there exists a broad region in which alumina and TiO_2 are stable phase at temperatures slightly lower than 1573 K (1300 °C), which agrees with the results of the present research. As there is no experimental data for this system at 1573 K (1300 °C), the discrepancy probably indicates that the thermodynamic modeling parameter should be further optimized. Furthermore, the changing behavior of homogeneous Al-Ti oxides to heterogeneous ones was also found to occur during heating at 1273 K (1000 °C), and it will be reported in our future work.

Alumina inclusion deteriorates the strength and toughness of steel products due to its hardness and high melting temperature. Industrially, the heating temperature and time should be controlled for Al-Ti–deoxidized steels to avoid unfavorable precipitation of alumina from the original oxides in as-cast alloys. Further study on the effect of heating temperature and time on evolution behavior of Al-Ti oxide inclusions should be conducted. However, in the present research, 3 hours was found to be enough time for alumina to precipitate during heating. On the other hand, this is attributed to the technology of "oxide metallurgy," employing oxides to enhance strength and toughness of steel by inducing intragranular acicular ferrites (IAFs), as first proposed by Japanese researchers.[15] It has been widely adopted to the production of heavy plates used for shipbuilding, offshore platforms, *etc.*, as oxides can refine the microstructure in the high heat-affected zone during welding.[16] Though Al-Ti oxide serving as a potential catalyst to IAF formation directly has not been reported, it has been proved that the induction mechanism is achieved by absorption of Mn ions from metal into vacancy of this oxide to produce a Mn depletion zone around oxide inclusion, which, in turn, increases the transformation temperature to promote acicular ferrite nucleation.[16–20] Jiang *et al.*[17] suggested that the chemistry of Al-Ti oxide is a great factor generating IAF through this mechanism, proved by laboratory and industrial experimental results. Recently, Cai *et al.*[20] found that the precipitation of MnS increased with an improvement of the Al/Ti molar ratio of the homogeneous Al-Ti oxide inclusions in water-quenched as-cast alloys, which results in a high fraction of IAF microstructure. However, the Al/Ti molar ratio of Al-Ti oxide is found to vary during the heating process, resulting in the possible loss of the effective nucleus of inducing IAF until the final steel products.

IV. CONCLUSIONS

The behavior of Al-Ti oxide inclusion was studied during 3-hours isothermal heating at 1573 K (1300 °C) in two alloys with different Al/Ti molar ratio. The conclusions are as follows.

1. Al-Ti oxide inclusions were characterized in both as-cast alloys. They were spherical and the size of most oxides was less than 1 μm. The chemistry showed homogeneous and the Al/Ti molar ratio of

these inclusions was consistent with that of alloy in both as-cast alloys.
2. After heating, most of homogeneous Al-Ti oxide inclusions changed to heterogeneous inclusions with Al-rich part and Ti-rich part while the remaining homogeneous oxides were found to be rare in both alloys. The concentration gradient of Al and O was observed inside the heterogeneous inclusion. The size distribution extended broader and the shape changed to irregular.
3. The mechanism of the variation was proposed to be the precipitation of alumina from homogeneous oxide inclusion during heating.

REFERENCES

1. F. Ruby-Meyer, J. Lehmann, and H. Gaye: *Scand. J. Metall.*, 2000, vol. 29, pp. 206–12.
2. I. Jung, S.A. Decterov, and A.D. Pelton: *ISIJ Int.*, 2004, vol. 44, pp. 527–36.
3. I. Jung, G. Eriksson, P. Wu, and A.D. Pelton: *ISIJ Int.*, 2009, vol. 49, pp. 1290–97.
4. H. Matsuura, C. Wang, G.H. Wen, and S. Sridhar: *ISIJ Int.*, 2007, vol. 47, pp. 1265–74.
5. C. Wang, N.T. Nufher, and S. Sridhar: *Metall. Mater. Trans. B*, 2009, vol. 40B, pp. 1005–21.
6. C. Wang, N.T. Nufher, and S. Sridhar: *Metall. Mater. Trans. B*, 2009, vol. 40B, pp. 1022–34.
7. C. Wang, N.T. Nufher, and S. Sridhar: *Metall. Mater. Trans. B*, 2009, vol. 41B, pp. 1084–94.
8. C. Wang, N. Verma, Y. Kwon, W. Tiekink, N. Kikuchi, and S. Sridhar: *ISIJ Int.*, 2011, vol. 51, pp. 375–81.
9. W. Choi, H. Matsuura, and F. Tsukihashi: *ISIJ Int.*, 2013, vol. 53, pp. 2007–12.
10. W. Choi, H. Matsuura, and F. Tsukihashi: *Metall. Mater. Trans. B*, 2016, vol. 47B, pp. 1851–57.
11. H. Matsuura, K. Nakase, and F. Tsukihashi: *CAMP-ISIJ,* 2010, vol. 23, p. 956 (CD-ROM).
12. E. Steinmetz, H.U. Linderberg, W. Morsdorf, and P. Hammerschmid: *Arch. Eisenhuttenwes*, 1977, vol. 48, pp. 569–74.
13. M. Nagano, S. Nagashima, H. Maeda, and A. Kato: *Ceram. Int.*, 1999, vol. 25, pp. 681–87.
14. The Japan Society for the Promotion of Science, The 19th Committee on Steelmaking: *Steelmaking Data Sourcebook,* Gordon and Breach Science Publications, New York, NY, 1988, pp. 279, 287, and 288.
15. J. Takamura and S. Mizoguchi: *Proceeding of the 6th International Iron and Steel Congress,* ISIJ, Nagoya, 1990, vol. 1, pp. 591–604.
16. S. Suzuki, K. Ichimiya, and T. Akita: *JFE Tech. Rep.*, 2005, vol. 5, pp. 24–29.
17. M. Jiang, X.H. Wang, Z.Y. Hu, K.P. Wang, C.W. Yang, and S.R. Li: *Mater. Charact.*, 2015, vol. 5, pp. 24–29.
18. Q. Huang, X. Wang, M. Jiang, Z. Hu, and C. Yang: *Steel Res. Int.*, 2015, vol. 87, pp. 445–55.
19. Z. Yang, F. Wang, S. Wang, and B. Song: *Steel Res. Int.*, 2008, vol. 79, pp. 390–95.
20. Z. Cai, Y. Zhou, L. Tong, Q. Yue, and H. Kong: *Mater. Testing*, 2015, vol. 57, pp. 649–54.